Identifying the Air Gun Bubble Pulse Event

By
Robert W. Lankston
March 14, 2017

A burst of energy referred to as the bubble pulse is generated whenever an explosion occurs under water. Actually, multiple pulses may be generated at predictable intervals. This phenomenon is discussed in geophysics textbooks that include a section on marine exploration seismic methods and on various websites and will not be repeated here.

In the case of the 1970 Flathead Lake seismic survey, the air gun was deployed approximately 1 m below the surface of the lake based on a photo provided by Richard Wold, co-principal investigator on the project. Figure 1 shows the pontoon from which the air gun was suspended, the metal harness that held the air gun, and the air gun assembly itself.

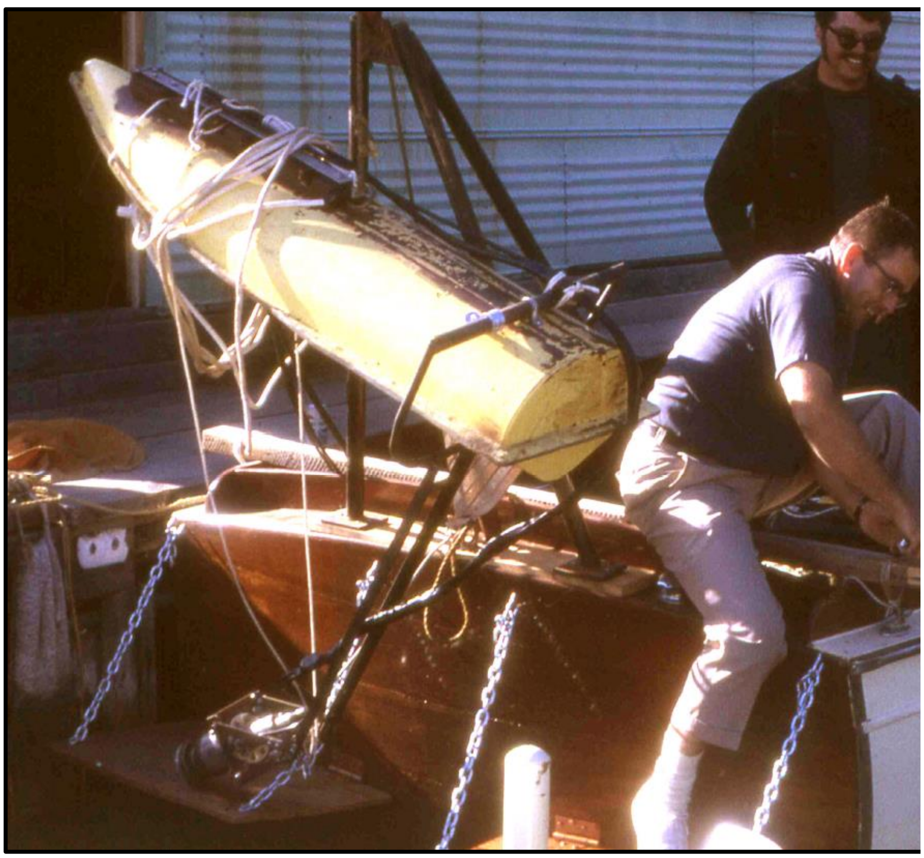

Figure 1. Air gun pontoon and suspension harness. The pontoon is the yellow item. The suspension harness is at the stern (right end) of the pontoon. The air gun itself is on the step on the stern of the survey boat in the lower left of the image. Original photograph courtesy of Richard Wold.

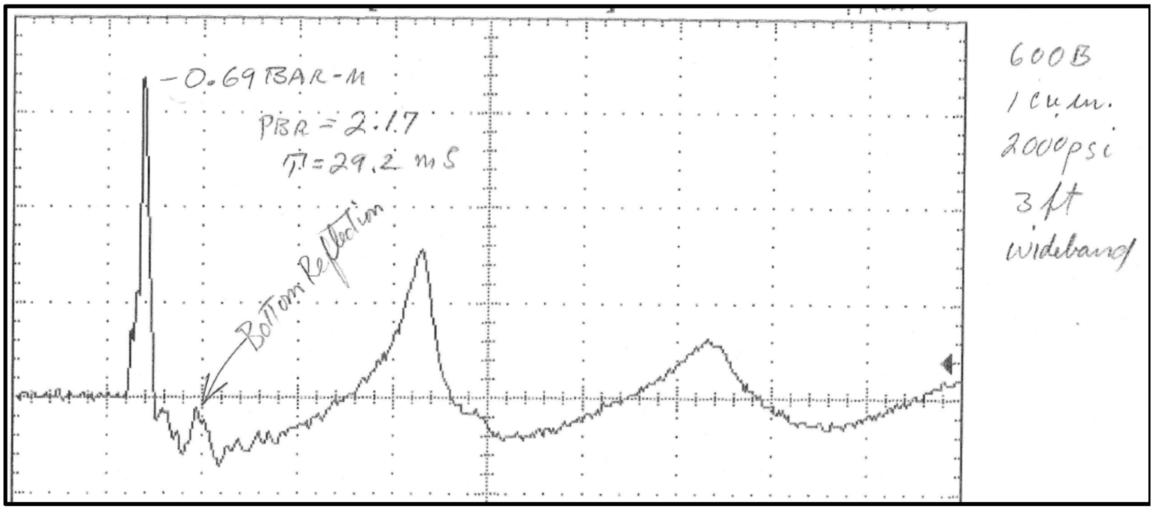

Figure 2. Air gun bubble wave train. The timing (vertical, dotted) lines are 10 ms apart. The zero amplitude level is the solid, horizontal line with tic marks at 2 ms intervals. The air gun discharge is the sharp peak at the left of the signal tracing. Two bubble events follow the discharge time by 29 and 58 ms, respectively. The onset of the third phase of the bubble wave train can be seen at the right edge of the tracing.

Chelminski (2011) of Bolt Technology Corporation, the manufacturer of the air gun that was used during the 1970 survey, provided the oscilloscope screen capture in Figure 2. In this 2005 experiment, the air gun was discharged at a depth of 3 ft below the surface, a depth similar to what would be expected in the Flathead Lake seismic survey. Chelminski's hand written annotations indicate that the first phase of the bubble wave train occurs 29 ms after the air gun discharge. A second phase of the bubble energy is also captured in the Figure 2 image at 29-30 ms after the first bubble phase. The amplitude of the bubble energy diminishes with each cycle as can be seen in Figure 2.

When working only with paper seismic sections, as would have been the case in the early days of the 1970 Flathead Lake seismic project, features such as multiples and the bubble pulse would have been identified by using drafting dividers or, possibly, an engineer's scale.

Figure 3 is a portion of Line F displayed from the data that survived on magnetic tape.[1] Double headed arrows in Figure 3, labeled a, b, c, and d, indicate primary reflections (tops of arrows) and the first phase of the bubble pulse that follows the respective primary reflections (bottoms of arrows). The double headed arrows attempt to illustrate the process of using a divider. For example, the divider would be set to the span of time between a primary event and the suspected bubble pulse at a point, say, a.

[1] The discovery of the tape and the digitization of the analog signals are described in Lankston (2007).

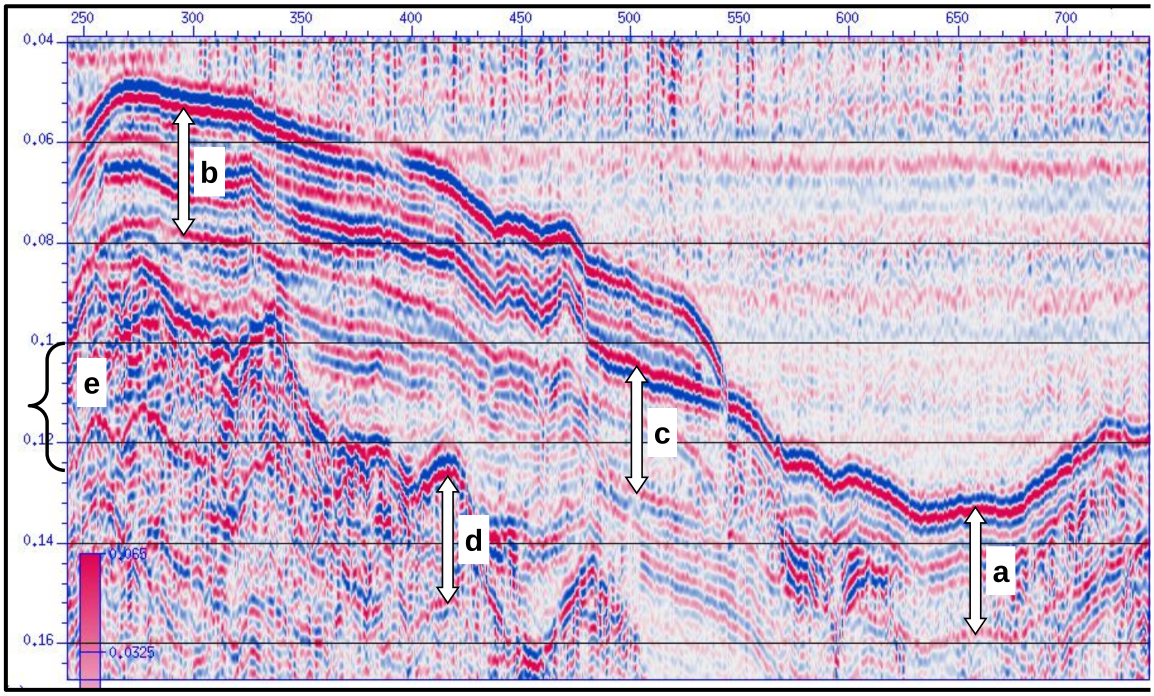

Figure 3. Line F with examples of bubble pulse events. The data are from a segment of Line F. The degree of saturation of the red (or blue) color is an indication of signal amplitude. Fully saturated red is the maximum positive amplitude while paler shades of red are lower amplitude. White is zero amplitude. Blue colors are negative amplitudes. The labels at the top are shotpoint numbers, and shotpoints are approximately 10 m apart, i.e., this display covers approximately 5000 m of survey line. The vertical axis is time in seconds with timing lines at 20 ms intervals. If the time axis were converted to depth using a linear time to depth transform of 1500 m/s, the depth range of this section would be approximately 100 m. Therefore, the vertical exaggeration of geologic details would be approximately 50:1. The significance of each of the cases, labeled a, b, c, d, and e, is in the text. The first phase of the bubble wave train in these examples follows the primary reflection by approximately 25 ms.

Keeping the divider spacing fixed (or the length of the arrow fixed as in Figure 3), one would test other locations such as b, c, and so forth.

In Figure 3, a and b both indicate the time lag between the water bottom reflection and the bubble pulse following it. This bubble phase after the water bottom reflection can be traced almost continuously across this line and others. One might place the divider at the strong event labeled c and notice that a relatively strong signal follows it by the same amount of time seen at a and b. The primary event at c is a strong reflection within the sediments. In the cases of a, b, and c, the bubble events are probably obscuring true, primary reflections within the sedimentary section.

Case d shows the reflection from what is interpreted to be the Precambrian floor of the lake basin. This is a strong reflection and, in many cases, it is a relatively continuous event on the survey lines. At d, the corresponding bubble phase is obvious. Case e is indicated by the curly

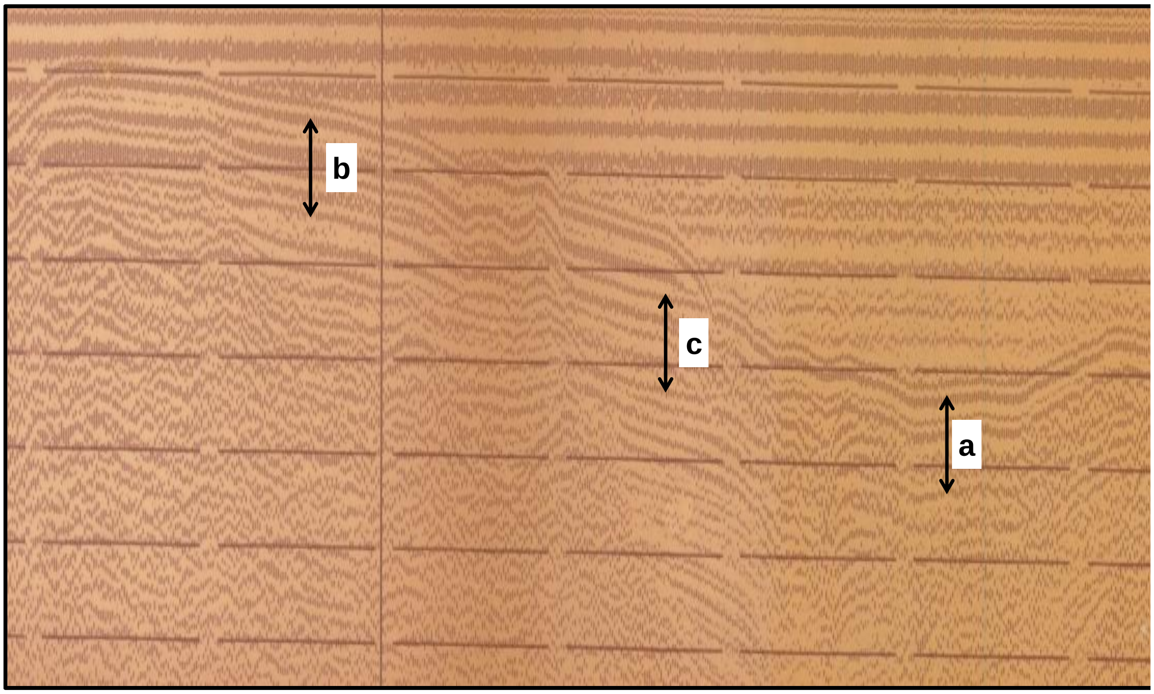

Figure 4. Original field recording of Line F. Timing lines are 25 ms apart. Cases a, b, and c are similar to a, b, and c in Figure 3. Without the help of an illustration such as Figure 3, the bubble pulse events might be mistaken for primary reflections. Because the facsimile style of recording loses all amplitude information, except for positive versus negative amplitude, the respective bubble events have essentially the same visual impact as the primary events.

bracket on the left. The bracket is plotted such that the time between the primary event and the first phase of the bubble energy can be scaled. In each of these cases, the time lag is 25 ms, very similar to the 29 ms illustrated in Figure 2. In measurements like this on other lines, the time lags varied from 25 ms to 30 ms.

With the monochrome displays of the early 1970's, identifying multiples and bubble pulses was not easy. Figure 4 shows a segment of the actual field recording for Line F. The segment is similar to that in Figure 3, and the scaling is also similar. With the experience of an analysis such as in Figure 3, one knows where to look for the bubble pulse event in the original recording.

The events labeled a, b, and c in Figure 4 are similar to a, b, and c in Figure 3. An advantage for identifying the bubble event in Figure 3 over Figure 4 is the color-coded amplitudes. The primary reflections (a, b, and c) in Figure 3 are fully saturated red indicating the maximum amplitude. The bubble events, however, are a lighter shade of red or pink indicating lower amplitudes.

The bubble phase is not limited to following the bright red events. In these data, the reflection events are usually a doublet, i.e., a peak-trough wavelet, with a bright blue immediately

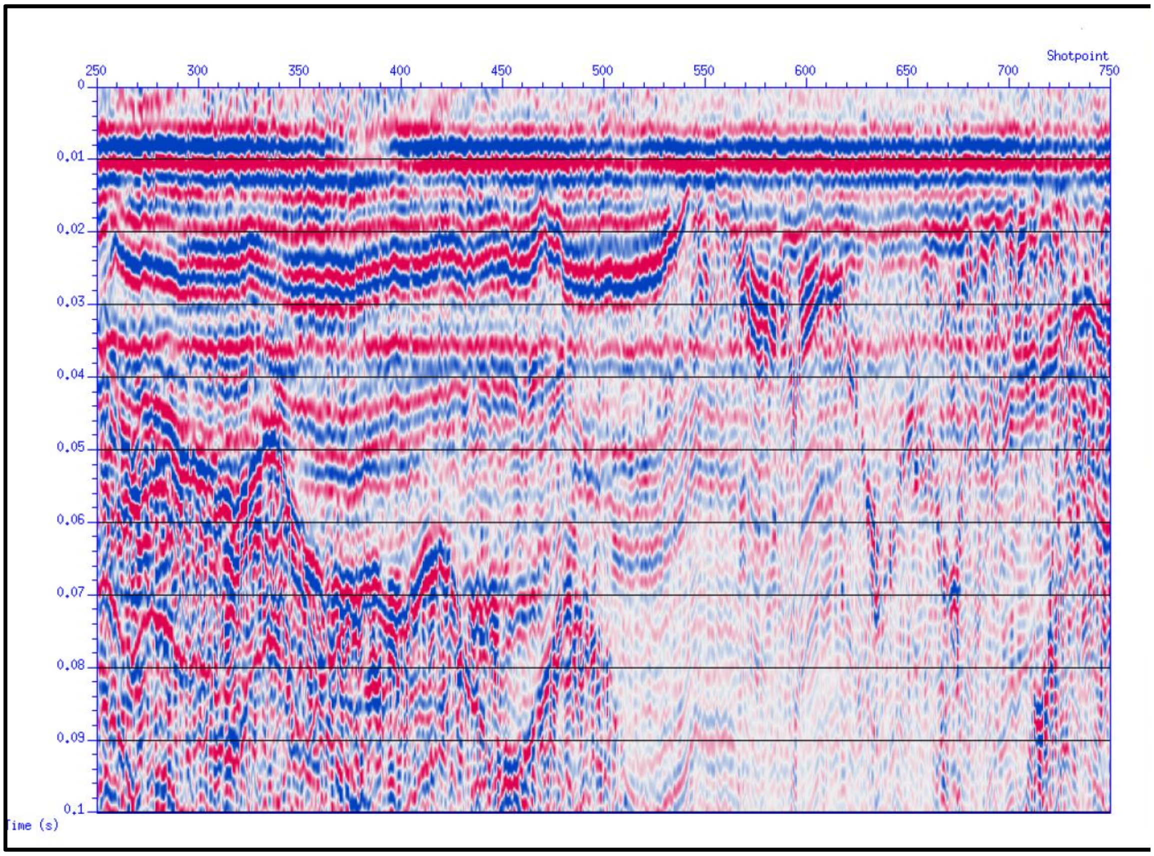

Figure 5. Portion of Line F flattened on the water bottom reflection. This is approximately the same set of traces as in Figure 3. The axis labels at the top are shotpoints, and shotpoints are approximately 10 m apart. The vertical axis is time in seconds with timing lines at 10 ms intervals. The water bottom reflection is the bright red event just below 10 ms. The first phase of the bubble wave train is at 35-36 ms, and it is essentially parallel to the flattened water bottom event.

following a bright red. The same red over blue doublet is seen in the interpreted bubble phases in Figure 3. The reds and blues of the bubble phases are lighter than the primaries, though, indicating amplitudes lower than the primary doublets.

With the availability of digital traces for lines such as F (Figure 3), one can now apply less manual, i.e., more automated, methods for gaining insight into the presence of multiples and bubble pulses. Recognizing that the water bottom event is strong and relatively continuous, one can use modern software to “pick” the water bottom horizon. Picking is the process of determining the arrival time of a specified event on a seismic trace. The picking process can be totally automatic with modern software if the event is distinctive, as the water bottom event is in this case.

Once the water bottom horizon is picked, software can “flatten” the horizon. The process of flattening applies a static shift to each trace such that all of the picked values occur along a horizontal time line. Figure 5 is the result of picking the water bottom event and flattening on that event. The flattened water bottom reflection is the strong horizontal event at slightly below 10 ms, an arbitrary datum level. Obvious in Figure 5 is an event 25-26 ms later that is essentially parallel to the flattened water bottom reflection and that is discordant with other events in the section. This is the first phase of the bubble pulse. The second phase of the bubble wave train should appear around 60 ms on the time scale in Figure 5. No horizontal signal alignment is evident around 60 ms suggesting that only the first phase of the bubble wave train is significant in this case.

Figure 5 is a useful display for analyzing one reflection and its bubble wave train. Another approach for discovering a repeating phase in the seismic section is to calculate the autocorrelation function for each trace. Autocorrelation, as employed in seismic data processing, is discussed in many geophysics textbooks.

Autocorrelation is the mathematical process of cross correlating a seismic trace with itself. The result is a measure of the similarity of the basic signal with time shifted versions of itself. Figure 6 is the set of autocorrelation results for the same set of traces displayed in Figure 3 (and Figure 5). For each trace in Figure 6, at time shift 0, the basic trace is compared to itself with no time shift, i.e., the similarity is perfect, and the result is the maximum possible value, in this case, normalized to 1, which is the bright red stripe at the 0 time line.

As each trace is shifted downward with respect to the unshifted version of itself, all of the primary reflections, regardless of their amplitudes, ultimately align with their respective bubble pulse counterparts. This gives a good similarity calculation but not perfect as in the zero shift case because the bubble phases are lower amplitude than their respective primary events. Because the bubble event is always the same time lag after every primary reflection, we see a pale red or pink horizontal line at 25-26 ms in the display (Figure 6). Important to note here is that this display is not dependent on one particular reflection, such as the water bottom reflection in Figure 5. Figure 6 is giving us a statistical sense of the time lag between every primary reflection and its bubble pulse.

The first phase of the bubble wave train that follows strong reflections, such as those in Figure 3, is easy to identify, particularly with modern tools. However, the bubble energy is not limited to the strong primary reflections. The bubble energy follows every primary reflection, regardless of amplitude, by the same amount of time lag. Because of this predictability, a process of deconvolution, such as is discussed in "Redisplay of the 1970 Flathead Lake Seismic Data" (Lankston, 2017) on this site, can be applied in an attempt to remove the offending noise phases and reveal true reflections that might have been obscured previously.

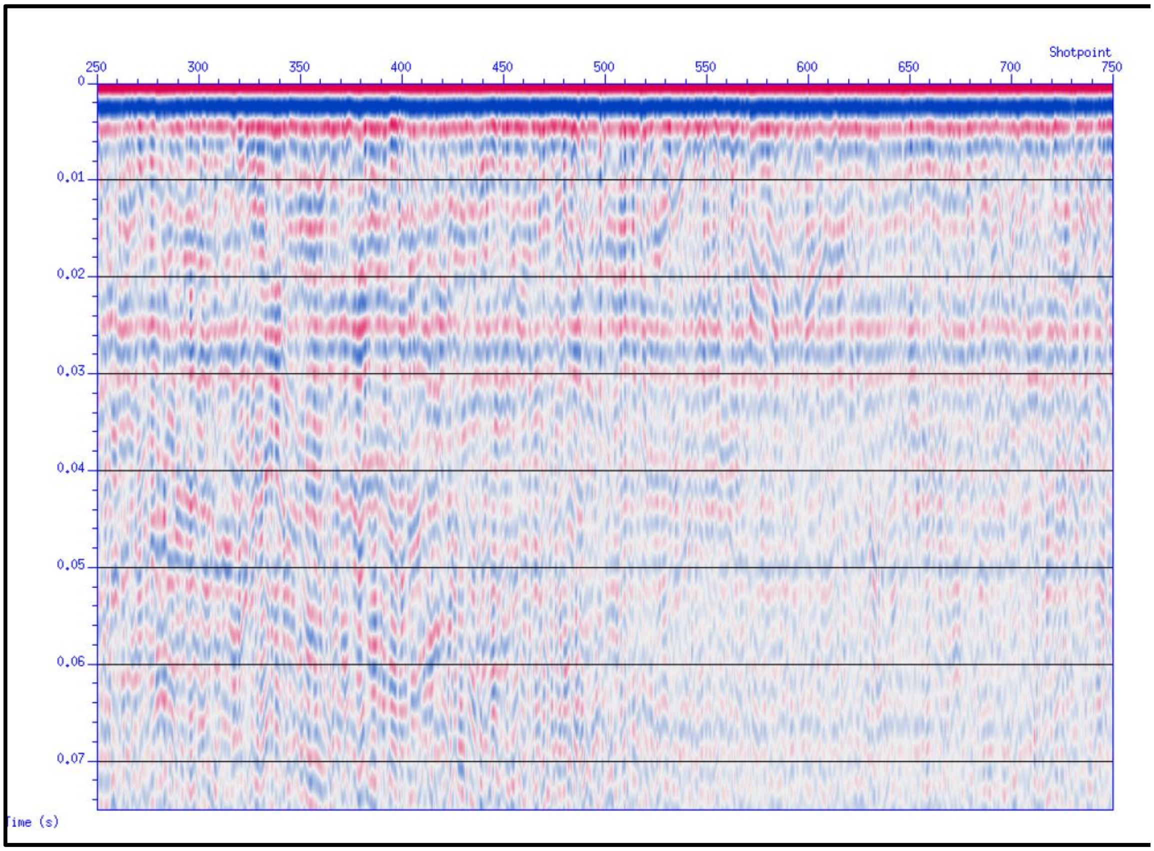

Figure 6. Autocorrelation of Line F traces. This is the same set of traces that was flattened on the water bottom event (Figure 5). Timing lines are at 10 ms intervals. The first phase of the bubble wave train is at 25–26 ms.

References Cited

Chelminski, P., 2011, personal communication.

Lankston, R. W., 2007, Revisiting the 1970 Flathead Lake seismic survey: The Leading Edge, v. 26, n. 8, p. 1058-1063.

Lankston, R. W., 2017, Identifying the air gun bubble pulse event, in J. New display of the 1970 Flathead Lake seismic data, http://scholarworks.umt.edu/flathead/13 .

Last update: 5/29/2023 7:46 PM